

## Absolute Instability of a Liquid Jet in a Coflowing Stream

Andrew S. Utada,<sup>1</sup> Alberto Fernandez-Nieves,<sup>1,\*</sup> Jose M. Gordillo,<sup>2</sup> and David A. Weitz<sup>1,3,†</sup>

<sup>1</sup>*School of Engineering and Applied Sciences, Harvard University, Cambridge, Massachusetts 02138, USA*

<sup>2</sup>*Área de Mecánica de Fluidos, Departamento de Ingeniería Energética y Mecánica de Fluidos, Universidad de Sevilla, Avenida de los Descubrimientos s/n 41092 Sevilla, Spain*

<sup>3</sup>*The Physics Department, Harvard University, Cambridge, Massachusetts 02138, USA*

(Received 13 July 2007; published 11 January 2008)

Cylindrical liquid jets are inherently unstable and eventually break into drops due to the Rayleigh-Plateau instability, characterized by the growth of disturbances that are either convective or absolute in nature. Convective instabilities grow in amplitude as they are swept along by the flow, while absolute instabilities are disturbances that grow at a fixed spatial location. Liquid jets are nearly always convectively unstable. Here we show that two-phase jets can breakup due to an absolute instability that depends on the capillary number of the outer liquid, provided the Weber number of the inner liquid is  $>O(1)$ . We verify our experimental observations with a linear stability analysis.

DOI: 10.1103/PhysRevLett.100.014502

PACS numbers: 47.61.Jd, 47.27.nf, 47.27.wg, 47.55.db

A thin stream of a Newtonian fluid is always unstable to breakup into drops, due to the surface-tension-driven Rayleigh-Plateau instability [1,2]. If the fluid is forced through an orifice, drop formation can occur either right at the exit or further downstream, at the end of a jet of fluid. These represent two regimes of the instability, dripping and jetting [3,4]. They are familiar to anyone who has watched water drip or flow from a faucet. Dripping is a common example of an absolute instability [5–9]; the perturbations that lead to drop pinch-off grow at a fixed location in space and at a frequency that is intrinsic to the system, making it insensitive to external noise [10]. As a result, monodisperse drops are almost always produced through a dripping instability [5–7]. By contrast, jetting is virtually always the result of a convective instability [11,12]; the perturbations that lead to jet breakup amplify random noise as they are advected along the interface of the jet, inevitably leading to less uniform drops. One means of generating highly uniform drops in the jetting regime would be to establish an absolute instability. This would be of significant scientific interest, and also of great value for technologies that require highly uniform drop formation, such as microfluidics [13,14], emulsification [15,16], and encapsulation [15]. However, absolute instabilities in the jetting regime have only been observed in the rarified environment of microgravity [17,18]. Despite their great technological potential and scientific interest, they have never been observed in liquid jets surrounded by a second viscous liquid.

In this Letter we report the observation of jets in a coflowing stream that break up into drops due to an absolute instability. We use a microcapillary device and identify characteristics of the jet shape and breakup that indicate an absolute instability. We further show that by increasing the shear stress on these jets above a critical value, the instability transitions from absolute to convective. We confirm the interpretation of our experimental results using a linear stability analysis.

We generate the jets in coflowing liquids using a capillary-based microfluidic device consisting of two coaxially aligned cylindrical capillaries housed within a larger square tube. We achieve good alignment of the cylindrical capillaries within the square tube by matching their outer diameters to the inner dimension of the square tube. We taper the tip of one of the inner capillaries to a diameter of  $d_{\text{tip}} \approx 30 \mu\text{m}$  and insert it into the second untapered capillary, which has an inner diameter of  $D \approx 600 \mu\text{m}$  and a length of  $\sim 5 \text{ cm}$ ; a schematic of the tapered tip is shown in the inset of Fig. 1(a). The outer liquid is poly(dimethylsiloxane) (PDMS) oil with a viscosity,  $\eta_{\text{out}} = 10 \text{ mPa} \cdot \text{s}$ , while the inner liquid is deionized water

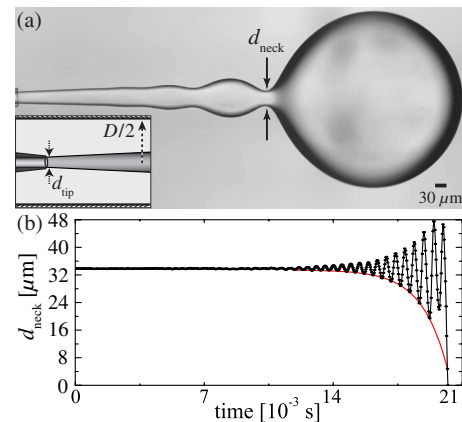


FIG. 1 (color online). (a) High-speed image of a typical jet. The small neck between the jet and the bulb has a diameter,  $d_{\text{neck}}$ . The outer diameter of the tip is  $\sim 40 \mu\text{m}$ , while  $d_{\text{tip}} \approx 30 \mu\text{m}$  and the inner diameter of the surrounding cylindrical capillary is  $\sim 600 \mu\text{m}$ . Here  $\mathcal{W}_{\text{in}} = 5.5$ . (Inset) Device schematic (not to scale). (b) Neck diameter as a function of time. The line is an exponential fit to the envelope. The frequency of drop formation is  $\sim 40 \text{ Hz}$  and the frequency of oscillation  $\sim 2000 \text{ Hz}$ . The flow rates of the outer and inner fluids are  $9 \times 10^4 \mu\text{L/hr}$  and  $6 \times 10^3 \mu\text{L/hr}$ , respectively.

with  $\eta_{\text{in}} = 1 \text{ mPa} \cdot \text{s}$ . The surface tension between the fluids is  $\gamma = 40 \text{ mN/m}$ , as measured by the pendant-drop method [19]. We drive each fluid with a syringe pump and image the jet with a high-speed camera. We note that gravitational forces are not relevant in our experiments as all characteristic length scales are well below the capillary length.

One common way of forming a jet in a coflow is to increase the outer flow rate, which increases the capillary number of the outer fluid,  $\mathcal{C}_{\text{out}} = \eta_{\text{out}} u_{\text{out}} / \gamma$ , where  $u_{\text{out}}$  is the mean velocity of the outer fluid. This number defines the balance of viscous shear forces to surface tension forces. Instead, we generate jets by injecting the inner fluid at a velocity large enough that inertial forces overcome surface tension forces at the exit of the tip [20]. This balance of forces is defined by the inner Weber number,  $\mathcal{W}_{\text{in}} = \rho_{\text{in}} L u_{\text{in}}^2 / \gamma$ , where  $\rho_{\text{in}}$  is the density of water,  $L$  is a characteristic length scale equal to the diameter of the jet, and  $u_{\text{in}}$  is the mean velocity of the inner fluid. At the exit of the capillary tip  $L = d_{\text{tip}}$  and we calculate  $u_{\text{in}}$  as the volume flow rate of the inner fluid divided by the cross-sectional area of the jet. In coflowing streams, jetting occurs when  $\mathcal{W}_{\text{in}} \gtrsim O(1)$  at the exit of the capillary [20]. In our experiments, the inner Reynolds number,  $\mathcal{R}_{\text{in}} = \rho_{\text{in}} L u_{\text{in}} / \eta_{\text{in}}$  is  $\sim O(50)$ , while the outer Reynolds number,  $\mathcal{R}_{\text{out}} = \rho_{\text{out}} D u_{\text{out}} / \eta_{\text{out}}$ , is  $\sim O(1)$ , where  $\rho_{\text{out}} = 960 \text{ kg/m}^3$  is the density of PDMS oil. Although jetting of a liquid in air also occurs at similar  $\mathcal{W}_{\text{in}}$  [3,4], the shape of the jets is dramatically different from those generated by the coflow. A water jet falling from a faucet under gravity becomes thinner along its length. By contrast, here we observe jets whose diameter increases along their length; this is a result of the viscous liquid surrounding the jet, as shown in Fig. 1(a). Further downstream, these jets develop a remarkable standing-wave-like oscillation that modulates the diameter; these oscillations are similar in appearance to capillary waves that form on jets due to gradients in surface tension [21]. However, the spatial undulations that we observe, although initially static, eventually begin pulsing radially and this ultimately leads to drop pinch-off; we provide a movie of the jet breakup in the supplemental information [22]. The resultant pulsing is most clearly seen in the neck of fluid that connects the jet to the growing bulb at its end; the neck diameter,  $d_{\text{neck}}$ , oscillates about its mean with an exponentially increasing amplitude until pinch-off occurs and the drop detaches, as shown in Fig. 1(b). Immediately following drop pinch-off, surface tension causes the end of the jet to retract, whereupon the next bulb begins to grow and the process repeats itself. Remarkably, throughout this entire process the spatial oscillations on the jet remain essentially stationary with respect to the flow of the inner fluid. We quantify this flow by measuring the mean velocity using tracer particles distributed homogeneously throughout the jet. The velocity within the jet can be as much as 100 times larger than the downstream velocity of the neck, as shown in Fig. 2(a).

The spatial oscillations on the jet and the fluid neck itself travel only a short distance downstream with a velocity comparable to  $u_{\text{out}}$  during the drop pinch-off process. At sufficiently large  $u_{\text{out}}$  the velocity of the neck and that of the particles become comparable [Fig. 2(a)].

The temporal pulsing and the nearly spatially stationary oscillations of the diameter are highly unusual behavior for jet breakup at moderate Reynolds numbers. More typically, when a thread of one fluid breaks within a second, the minimum thread diameter decreases to zero at pinch-off without oscillations of any sort [23,24], although oscillations have been observed in a numerical simulation [25]. To understand the temporal oscillations of the jet, which remain nearly stationary in space, we turn to linear stability theory: we decompose the perturbations on the jet into Fourier modes, assumed to be axisymmetric. Any parameter associated with the flow, such as the velocity or pressure, is defined to be proportional to  $e^{i(kz - \omega t)}$ , where  $z$  is the axial coordinate and  $t$  is time. In general, the frequency,  $\omega = \omega_r + i\omega_i$ , and wave number,  $k = k_r + ik_i$ , of the perturbations are complex and are related through a dispersion relation of the form  $D(\omega, k) = 0$  [10]. The superposition of the different modes generates wave packets that travel both up and downstream along the interface of the jet, with group velocity,  $v_{\text{group}}$ . Typically, a temporal stability analysis is used to determine whether or not a system is stable by examining the behavior of the perturbations over time. In this analysis, the wave number is assumed to be real,  $k = k_r$ , to separate temporal from spatial instability. If the growth rate of the instability is  $\omega_i < 0$ , then the perturbations decay in time and the system is stable and jet breakup will not occur; by contrast, if  $\omega_i > 0$ , the perturbations grow exponentially, making the system unstable and drop pinch-off can occur. In this case, this analysis is

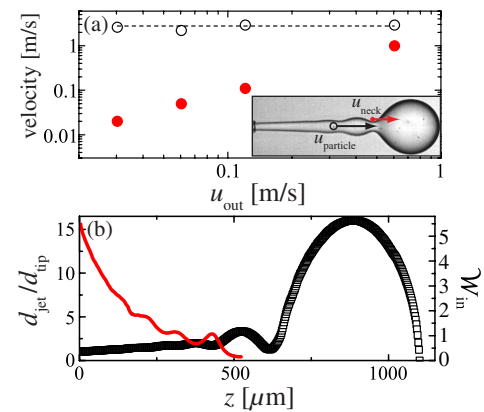


FIG. 2 (color online). (a) Downstream velocities of the neck (filled circles),  $u_{\text{neck}}$ , and  $6 \mu\text{m}$  tracer particles (open circles),  $u_{\text{particle}}$ , dispersed in the inner fluid as a function of the velocity of the outer fluid. The dashed line is the mean velocity of the inner fluid at the exit of the capillary tip. (inset) Image of a jet containing dispersed particles. (b) The profile of the jet shown in Fig. 1(a) (open squares) and the  $\mathcal{W}_{\text{in}}$  (line) as a function of the axial position along the jet.

followed by a spatiotemporal analysis that distinguishes convective from absolute instabilities. This distinction is made based on the Briggs-Bers criterion, which requires finding specific  $\omega_0$  and  $k_0$  that satisfy  $D(\omega_0, k_0) = 0$  and  $v_{\text{group}} = \frac{\partial \omega}{\partial k} \Big|_{\omega=\omega_0, k=k_0} = 0$ , at a specific spatial location in the laboratory frame of reference [10]; physically, this condition can be qualitatively interpreted to occur when the upstream velocity of the wave packet coincides with the downstream velocity of the interface. If the imaginary part of  $\omega_0$  is negative, the instability is convective since the perturbations decay with time at the specified location. By contrast, if the imaginary part of  $\omega_0$  is positive, the instability is absolute since the perturbations grow exponentially with time at the specified location.

In our experiments, the amplitude of the oscillations at the neck that lead to drop pinch-off grow exponentially in time [Fig. 1(b)], implying that the growth rate of the instability is positive. In addition, the large difference in velocity between the neck and  $u_{\text{in}}$  [Fig. 2(a)] coupled with the spatially stationary oscillations throughout the entire pinch-off process suggests that the superposition of the perturbations produces the condition of  $v_{\text{group}} = 0$  at a fixed spatial location. Further insight into the breakup of these jets can be gained by examining the decrease of  $\mathcal{W}_{\text{in}}$  along the axis of the jet. Although, we generate these jets by injecting the inner fluid at  $\mathcal{W}_{\text{in}} > O(1)$ , drop pinch-off from the end of the jet occurs only after the jet diameter has widened sufficiently such that  $\mathcal{W}_{\text{in}}$  decreases to  $\sim 1$ ; this decrease is shown by the line superimposed on the jet profile in Fig. 2(b). Since dripping occurs only when  $\mathcal{W}_{\text{in}} \lesssim O(1)$  [3,4] we hypothesize that the drop pinch-off mechanism from the widening jets is analogous to the dripping regime, at the end of the jet. These characteristics strongly suggest that the widening jets breakup due to an absolute instability [6,8,9].

As a further test of our interpretation, we increase the shear stress on the jet to upset the balance between the interface velocity and the upstream velocity of the wave packet; this corresponds to a transition from an absolute to a convective jet instability. Since the interface velocity is controlled mainly by the outer fluid, the relevant metric for this transition is  $C_{\text{out}}$ . In these experiments, we achieve a factor of 10 increase in  $C_{\text{out}}$  by increasing  $\eta_{\text{out}}$  from 10 to 100 mPa · s. We start by generating a jet at  $\mathcal{W}_{\text{in}} = 3.1$  with  $C_{\text{out}} \ll 1$ , and gradually raise  $C_{\text{out}}$  by increasing  $u_{\text{out}}$ ; an image of this jet before we increase  $u_{\text{out}}$  is shown in Fig. 3(a). In this particular case the jet breakup process leads to drops of two different sizes; following the detachment of the larger drop, a second smaller drop detaches from the neck as it retracts, as has been observed in other systems [26–28]. Increasing  $C_{\text{out}}$  by nearly a decade produces no significant change in the jet length,  $L_{\text{jet}}$ ; however, at a critical  $C_{\text{out}}^* \approx 0.65$  we observe an abrupt and dramatic increase in  $L_{\text{jet}}$ , as shown in Fig. 3(b) and 3(c). The corresponding measurements of jet length are shown as filled squares in Fig. 3(d); we label the points referring to

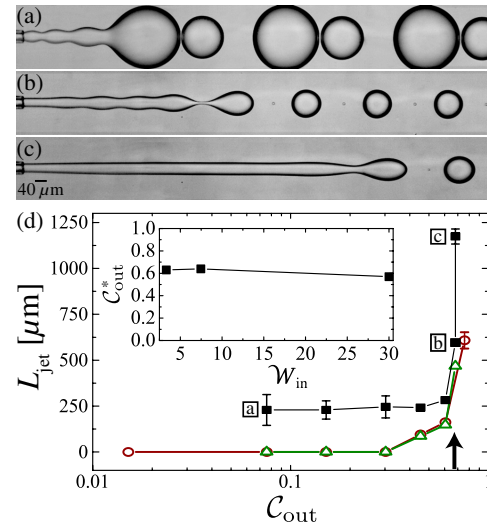


FIG. 3 (color online). Jet length as a function of  $C_{\text{out}}$ . (a) Image of the jet generated at  $\mathcal{W}_{\text{in}} = 3.1$  and  $C_{\text{out}} = 0.07$ . (b) Transient image of the jet generated at  $C_{\text{out}} = 0.69$ . The oscillations on the jet gradually die out as the length increases at the critical value,  $C_{\text{out}}^*$ . (c) Image of the jet at  $C_{\text{out}} = 0.69$  after the lengthening. (d) Plot of the jet length as a function of  $C_{\text{out}}$ . The filled squares are the measured jet lengths. The data points corresponding to (a)–(c) are labeled. The open circles and triangles are dripping, where  $L_{\text{jet}} = 0$ . The  $\mathcal{W}_{\text{in}}$  for the circles and triangles is 0.19 and 0.05, respectively. The arrow marks  $C_{\text{out}}^*$  obtained from the linear stability analysis. Inset: Linear stability analysis. Below  $C_{\text{out}}^*$  the jet breaks due to an absolute instability, while above, it breaks due to a convective instability. For these experiments  $\eta_{\text{in}}/\eta_{\text{out}} = 0.01$ .

the images in Fig. 3(a)–3(c) with the appropriate letter. Remarkably, this large increase of  $L_{\text{jet}}$  also coincides with the suppression of the spatial oscillations as the jet evolves in time [Fig. 3(b) and 3(c)].

We can quantitatively describe this transition using our linear stability analysis. We first calculate the downstream evolution of the velocity profiles of both fluids [29,30]. The velocity profile of the inner liquid is parabolic as it emerges from the tip and gradually flattens downstream due to the widening of the jet, while the velocity profile of the outer liquid is nearly parabolic although a thin boundary layer develops near the jet [31]. We then perform a spatial stability analysis under these flow conditions by determining the sign of the imaginary part of  $\omega_0$  at several axial positions along the jet [10,30]. We find that below a calculated value of  $C_{\text{out}}^* = 0.69$ , the jets are absolutely unstable within a section of the jet that is much larger than the characteristic wavelength of the absolute mode,  $\lambda_0 = 2\pi/k_0$ ; since this section is much larger than  $\lambda_0$ , this mode can grow, resulting in jet breakup due to an absolute instability. Above  $C_{\text{out}}^*$ , however, the absolutely unstable section is located immediately adjacent to the tip and is greatly reduced in spatial extent. In this case, since the absolutely unstable section is very small compared to  $\lambda_0$ , the absolute mode can no longer grow, resulting in jet

break up due to a convective instability. Furthermore, this calculated value of  $C_{\text{out}}^*$  is in remarkably good agreement with our experimental observations.

Our linear stability analysis further predicts that the value of  $C_{\text{out}}^*$  does not change significantly as a function of  $\mathcal{W}_{\text{in}}$  [inset of Fig. 3(d)]; this implies that the shear from the outer liquid determines the transition from an absolute to convective instability irrespective of the inertia of the inner liquid. This prediction is consistent with our data, which show that nearly the same  $C_{\text{out}}^*$  that causes the abrupt jet lengthening when  $\mathcal{W}_{\text{in}} = 3.1$  also induces a similar transition when  $\mathcal{W}_{\text{in}} \ll 1$ , as shown by the open symbols in Fig. 3(d). This is remarkable because when  $\mathcal{W}_{\text{in}} \ll 1$  and  $C_{\text{out}} < C_{\text{out}}^*$  the system is in a dripping regime; above  $C_{\text{out}}^*$ , however, the system transitions from an absolutely-unstable dripping regime [5–9] to a convectively unstable jetting regime. This emphasizes the analogies between the dripping and the widening-jet regimes, adding further support to our hypothesis that the increase in  $L_{\text{jet}}$  [Figs. 3(a)–3(c)] corresponds to a transition from an absolute to a convective instability.

Absolute instabilities are not widely observed in jet breakup due to the fine balance of forces required to generate them. The balance is difficult to achieve under gravitational acceleration, although it is possible in microgravity [17,18]. However, as we show here, in two-phase coflows, increasing  $\mathcal{W}_{\text{in}}$  above  $\sim 1$  to induce the formation of a widening jet [20] can also produce the appropriate conditions for an absolute instability to form. Although we discuss the transition of the instability from absolute to convective in terms of the two control parameters  $C_{\text{out}}$  and  $\mathcal{W}_{\text{in}}$ , there are two additional dimensionless parameters that we must consider to fully describe our system; these can be chosen as  $\eta_{\text{in}}/\eta_{\text{out}}$ , and the inner Ohnesorge number,  $\mathcal{O}_{\text{in}} = \frac{\eta_{\text{in}}^2}{\rho_{\text{in}} d_{\text{in}} \gamma}$ , which simply characterize material properties of the system and the experimental geometry. Altering these two parameters would most likely not affect the physical mechanism by which shear causes the transition from an absolute to convective instability but would likely only change the value of  $C_{\text{out}}^*$ . Nevertheless, through further exploration over the range of these four nondimensional numbers we can achieve an even greater understanding over the conditions leading to the development of absolute instabilities in two-phase systems. This could enable the tuning of the nature of the instability to offer another route to generate uniform emulsions from jet breakup.

This work was supported by the NSF (No. DMR-0602684) and the Harvard MRSEC (No. DMR-0213805). We thank M.P. Brenner for helpful discussions. A.F.-N. thanks the University of Almeria (leave of absence) and Junta de Andalucía (No. FQM-3116).

<sup>†</sup>weitz@seas.harvard.edu

- [1] J. Plateau, Acad. Sci. Bruxelles Mém. **23**, 5 (1849).
- [2] L. Rayleigh, Proc. R. Soc. London **29**, 71 (1879).
- [3] C. Clanet and J.C. Lasheras, J. Fluid Mech. **383**, 307 (1999).
- [4] B. Ambravaneswaran, H. J. Subramani, S. D. Phillips, and O. A. Basaran, Phys. Rev. Lett. **93**, 034501 (2004).
- [5] J. M. Gordillo, A. M. Gañán-Calvo, and M. Pérez-Saborid, Phys. Fluids **13**, 3839 (2001).
- [6] A. Sevilla, J. M. Gordillo, and C. Martínez-Bazán, Phys. Fluids **17**, 018105 (2005).
- [7] A. Sevilla, J. M. Gordillo, and C. Martínez-Bazán, J. Fluid Mech. **530**, 181 (2005).
- [8] A. M. Gañán-Calvo and P. Riesco-Chueca, J. Fluid Mech. **553**, 75 (2006).
- [9] P. Guillot, A. Colin, A. S. Utada, and A. Ajdari, Phys. Rev. Lett. **99**, 104502 (2007).
- [10] P. Huerre and P. A. Monkewitz, Annu. Rev. Fluid Mech. **22**, 473 (1990).
- [11] J. Eggers, Rev. Mod. Phys. **69**, 865 (1997).
- [12] S. P. Lin and R. D. Reitz, Annu. Rev. Fluid Mech. **30**, 85 (1998).
- [13] H. A. Stone, A. D. Stroock, and A. Ajdari, Annu. Rev. Fluid Mech. **36**, 381 (2004).
- [14] M. Joanicot and A. Ajdari, Science **309**, 887 (2005).
- [15] G. T. Vladisavljevic and R. A. Williams, Adv. Colloid Interface Sci. **113**, 1 (2005).
- [16] V. Schmitt, F. Leal-Calderon, and J. Bibette, Top. Curr. Chem. **227**, 195 (2003).
- [17] I. Vihinen, A. M. Honohan, and S. P. Lin, Phys. Fluids **9**, 3117 (1997).
- [18] B. O'Donnell, J. N. Chen, and S. P. Lin, Phys. Fluids **13**, 2732 (2001).
- [19] F. K. Hansen and G. Rodsrud, J. Colloid Interface Sci. **141**, 1 (1991).
- [20] A. S. Utada, A. Fernandez-Nieves, H. A. Stone, and D. A. Weitz, Phys. Rev. Lett. **99**, 094502 (2007).
- [21] M. J. Hancock and J. W. M. Bush, J. Fluid Mech. **466**, 285 (2002).
- [22] See EPAPS Document No. E-PRLTAO-99-076753 for a movie showing jet breakup in our coflowing system. For more information on EPAPS, see <http://www.aip.org/pubservs/epaps.html>.
- [23] J. R. Lister and H. A. Stone, Phys. Fluids **10**, 2758 (1998).
- [24] I. Cohen, M. P. Brenner, J. Eggers, and S. R. Nagel, Phys. Rev. Lett. **83**, 1147 (1999).
- [25] C. Zhou, P. Yue, and J. J. Feng, Phys. Fluids **18**, 092105 (2006).
- [26] T. Thorsen, R. W. Roberts, F. H. Arnold, and S. R. Quake, Phys. Rev. Lett. **86**, 4163 (2001).
- [27] S. L. Anna, N. Bontoux, and H. A. Stone, Appl. Phys. Lett. **82**, 364 (2003).
- [28] P. Garstecki, M. J. Fuerstman, and G. M. Whitesides, Phys. Rev. Lett. **94**, 234502 (2005).
- [29] This is done using the method of lines as described in [30].
- [30] J. M. Gordillo and M. Pérez-Saborid, J. Fluid Mech. **541**, 1 (2005).
- [31] We neglect the presence of the bulb at the end of the jet in our analysis of the jet breakup. This is justified since we can change the size of the bulb by a factor of 2 by changing  $u_{\text{out}}$  without affecting the jet length and jet breakup mechanism.

\*Present address: School of Physics, Georgia Institute of Technology, Atlanta GA, 30332, USA.